JOURNAL OF SOLID STATE CHEMISTRY 36, 371–380 (1981)

The Structure of Quartz at 25 and 590°C Determined by Neutron Diffraction

A. F. WRIGHT AND M. S. LEHMANN

Institut Laue Langevin, 156X, 38042 Grenoble Cedex, France

Received March 24, 1980

Analysis of single-crystal data on the α to β transformation in quartz, which takes place at 573°C, showed that the model which, till now, has best agreed with available X-ray data, does not hold for the neutron data. In an earlier model both oxygen and silicon atoms move to special positions (6*j* and 3*c* in the space group $P6_222$). The new data for β-quartz were best explained by assuming a disorder for the oxygen atom around the 6*j* position, and in order to keep regular SiO_4 tetrahedra, a corresponding small disorder in the silicon atom is assumed.

Introduction

In an attempt to understand the anomalous thermal properties of β-quartz (stable above 573°C) an investigation of the structural changes with temperature up to 1000°C has been undertaken. High-resolution neutron diffraction has been obtained from powdered synthetic quartz and from single crystals of natural and synthetic quartz. We report here the results for a single temperature (590°C) characteristic of the β-phase, since our conclusions represent a significant departure from the classical structure for β-quartz. For completeness, we also report the structure of α-quartz at room temperature from data collected from the same synthetic crystal. In all cases, the β-quartz data are best described if we adopt a model in which the SiO_4 tetrahedra are disordered. The proposed disorder is a correlated spatial distribution of the SiO_4 tetrahedra about the ideal high-quartz structure with large displacements in the direction of the Dauphiné twin configurations α_1 and α_2 of low quartz.

Two most common types of twinning occur in quartz, Brazil twinning and Dauphiné twinning. The former has no observable effect on diffraction data, whereas the second leads to equality in the reflections F_{hkl} and F_{khl} which are not identical by symmetry. In a Dauphiné twin, crystal II is related to crystal I by a 180° rotation about the threefold axis. Reflection F_{hkl} of crystal I is then superimposed on reflection F_{khl} of crystal II, and given a volume fraction x of crystal II the observed intensity is given by (*1*)

$$|F_{hk\cdot l}|^2(\text{obs}) = x|F_{kh\cdot l}|^2_{\text{II}} + (1-x)|F_{hk\cdot l}|^2_{\text{I}}.$$

Since the twin configurations α_1 and α_2 are energetically equivalent at all temperatures, the twinning density is only limited by the excess energy of the twin boundary, but may be influenced by local effects such as impurities or surface strains, which direct the crystal or parts of it into one or the other configuration. Impure natural crystals are often composed of α_1 and α_2 regions such that $x \to 0.5$, whereas pure crystals

0022-4596/81/030371-10$02.00/0

are often monodomain except for minor regions at the surface.

Near the phase transformation, the density of Dauphiné twinning increases and a two-dimensional "lattice" of Dauphiné twins develops whose period decreases with increasing temperature. The effect has been observed by X-ray diffraction (*2*), by light scattering (*3*), and by electron microscopy. The single-crystal domains have the form of triangular prisms elongated parallel to the threefold axis. In view of the long-range order of the domain structure, Dauphiné twinning is regarded as a characteristic of the quartz structure. The role of Dauphiné twinning in the β-phase or in the mechanism of the phase transformation is not known. In the ideal β-quartz structure there is no Dauphiné twinning since the twin pairs are indistinguishable by symmetry at the displacive limit, but recent work suggests that the real β structure retains the α-quartz symmetry in a domain (*5*) or time-averaged (*4*) structure. The present work shows that in the $\alpha \rightarrow \beta$ phase transition, the high-symmetry displacive limit is not attained, but instead an averaged structure of the same symmetry results. The $\alpha \rightarrow \beta$ phase transition is therefore of the order–disorder type similar to that of cristobalite (*6*).

Experimental

(*I*) *Powder Diffraction*

Neutron powder diffraction profiles were obtained from ground synthetic quartz at 630°C on the high-resolution powder diffractometer D1A. The finely ground sample (supplied by Quartzkeramik, Stockdorf bei-München) was packed in a 1-cm-diameter vanadium can and mounted in a vacuum furnace with a vanadium foil heater. Data were collected over the 2θ range 20 to 140° at a wavelength of 1.909 Å in a period of 24 hr. The profiles from the 10 counters of the diffractometer were normalized and summed to give a single profile suitable for refinement by the method of Reitveld (*7*). The peaks were well resolved, enabling the rather flat background between peaks to be accurately subtracted. No correction for absorption was necessary.

(*II*) *Single-Crystal Diffraction*

Two crystals were used for measurements, one synthetic and one of natural origin. The synthetic crystal was a piece of a large single crystal (supplied by Quartzkeramik, Stockdorf bei-München) which broke when cooled from the β to the α phase. A specimen suitable for measurement was obtained by grinding a sphere of diameter 0.194 cm. Originally the large crystal was a single-domain crystal of optical quality. The natural crystal was taken from a conglomerate of crystals found by Drs. A. Heidemann and H. Egger near Chamrousse in the Belledonne mountain chain of the French Alps. In this case the sample was a hexagonal column with a length of 0.24 mm and a distance between opposite hexagonal faces of 0.17 cm. This crystal had a milky appearance.

Neutron diffraction data were collected at the four-circle diffractometer D9 located at the hot source of the Institut Laue Langevin high-flux beam reactor. The wavelength was 0.723 Å, and was chosen to be a compromise between good reflectivity for the crystal at the high temperatures and reduction of extinction, which was expected to be severe for the synthetic crystal. The monochromatic beam was obtained by reflection from the (200) planes of a Cu crystal in transmission geometry. Coupled ω–2θ step scans were used to record the reflection profiles in the bisecting geometry and the number of steps in each profile was 41. The step length was varied as a function of the Bragg angle, and in addition steps were larger in the background than in the peak. In general half the points were re-

cordings of background. The total scan width ranged from 2.6° at low angle to 3.10° at 70° in 2θ. The stability of the instrument was monitored by measurement of a standard reflection at intervals of 30 reflections. Second-order contamination was reduced to less than 0.2% by means of an ir filter.

Data were obtained at room temperature for the synthetic crystal and at 590°C for both crystals. The crystals were heated by a stream of hot air which arrives at the crystal along an axis coincident with the neutron beam (*8*). This is obtained by making the diameter of the gas nozzle large enough to allow the neutron beam to pass through the center without touching. No neutrons are scattered by the heating equipment. The heater was easily calibrated at the transition temperature of 573°C by observation of the change of extinction at the transition. This effect was observed over a range of several degrees, and can be ascribed partly to a small gradient over the crystal and partly to the fact that extensive changes in the mosaic structure do take place some degrees below the transition (*4*). The transition temperature was assumed to correspond to maximum extinction change. An estimate of the stability of the furnace was obtained from repeated measurements of reflection intensities at the transition, and it was found that temperature variations were less than a degree over several days.

For both crystals data were measured to a 2θ value of 70°, and it was ensured that for the room-temperature data at least two, and for the high-temperature data at least four, symmetry-related reflections were recorded. The Bragg reflection profiles for the natural crystal had large shoulders. In order to ensure that the scan gave a complete integration of the elastic intensity a set of data was collected using the ω–scan technique, which for small Bragg angles is a scan through reciprocal space nearly orthogonal in direction to the ω–2θ scan. Earlier measurements on the instrument using good-quality Cu crystals have shown that the scanning ratio between ω and θ that keeps the Bragg spot at the center of the detector surface during the scan is zero (ω scan) at low Bragg angles increasing to 2 (ω–2θ scan) for θ around 35°, so with a sufficiently large aperture a complete integration should be possible. Indeed, refinements of the two sets of data led to structural parameters that agreed within two standard deviations except for the scale factor, where the value was three standard deviations smaller for the ω scan than for the ω–2θ scan.

Profiles were reduced to F_0^2 values with the minimal $\sigma(I)/I$ criteria including a correction of the known bias in the method (*9*), where I is the integrated intensity and $\sigma(I)$ its standard deviation. No corrections were made for absorption, thermal diffuse scattering, and multiple scattering.

The numbers of reflections measured were 583 and 681 for the synthetic crystal at room temperature and 590°C, respectively, and for the natural crystal 677 reflections were recorded. After averaging of symmetry-related reflections there were 204 reflections at room temperature and 128 at high temperature. The disagreement index between symmetry-related squared-structure amplitudes was 0.026 for the natural crystal, and for the synthetic crystal the values were 0.014 at room temperature and 0.039 at 590°C. This decrease in agreement at high temperature is quite remarkable. It is partly due to a reduction in precision from reduced intensities at high angles, but also from lower agreement between symmetry-related reflections in the high-temperature phase. This disagreement could not be removed either by several passages through the transition, or by several days' heating at 800°C.

Powder Data Refinements

Since the powder profile is a representa-

tion of the sum of all crystal orientations, powder diffraction is insensitive to macroscopic twinning where each component diffracts as an individual crystal.

In a time-averaged or "microtwin" domain structure however, diffraction occurs from the average structure weighted according to the occupation of sites in each domain. We can thus discriminate between ideal ordered or "disordered" structures by refinement of the total or fractional occupancy of the atomic positions. Refinement of the powder profile was carried out according to the method of Rietveld (*7*), developed to include anisotropic thermal parameters by Hewat (*10*). The space group was assumed to be $P6_222$, which corresponds to adding a twofold axis to the threefold axis of the low-temperature form. For the choice of the atomic positions we consider two possibilities. Young (*2*) suggested that both atoms are in special positions, Si in $3c$ ($\frac{1}{2}$, 0, 0) and O in $6j$ ($2x$, x, $\frac{1}{6}$). By placing the three silicon atoms in $6j$ (x, 0, 0) and the six oxygen atoms in general positions, with an occupancy factor of $\frac{1}{2}$, we describe the diffraction from an average structure where the two local configurations corresponding to α_1 and α_2 twins are equally represented in the diffraction event. The ordered structure ($\alpha_1 \equiv \alpha_2$) is of course implicitly included as a limiting case of this model. The quantity minimized in the Rietveld profile refinement is

$$\chi^2 = \Sigma_i w_i |y_i(\text{obs}) - (1/c)\, y_i\,(\text{calc})|^2,$$

where y_i (obs) and y_i (calc) are the observed and calculated intensities at $2\theta_i$, $w_i = 1/y_i(\text{obs})$ is the assigned weight, and c is the scale factor. Two R factors are calculated, the profile residual

$$R_p = \Sigma_i |y_i(\text{obs}) - (1/c)\, y_i\,(\text{calc})| / \Sigma_i y_i(\text{obs})$$

and a corresponding R factor for integrated intensities for comparison with single-crystal results or classical powder pattern analysis.

$$R_I = \Sigma_k |I_k(\text{obs}) - (1/c)\, I_k\,(\text{calc})| / \Sigma_k I_k(\text{obs}).$$

Neutron scattering lengths used were $b_{Si} = 0.415 \times 10^{-12}$ cm and $b_O = 0.58 \times 10^{-12}$ cm (*11*). Anisotropic thermal parameters were refined for oxygen, but considering the need to restrict the number of parameters in line with the limited data available from the powder profile, an isotropic thermal parameter was used for silicon. Since silicon is at the center of a regular tetrahedral arrangement, this represents a good approximation.

Refinement very strongly favored a disordered structure (Table I), with a large separation (0.4 Å) between equivalent oxygen atoms of the α_1 and α_2 domains, very much greater than the estimated limits of error (3σ for z, 6σ for y). The silicon atom also showed a small displacement from the ideal β-quartz position (0.06 Å) but at this stage it could not be considered significant, as in general all the standard deviations were relatively large. Confining the silicon atoms to x, $y = 0.5$ did not cause any significant increase in R_p. On the other hand all the refined parameters including the Si coordinates are remarkably close to those determined by Young for α-quartz in space group $P3_221$ below the phase transformation at 570°C. Refinements on data collected at other temperatures up to 1000°C confirmed all the structural features of the 630°C measurement, but additional structural trends with temperature which we hoped to see were not observed, presumably because such changes are small compared to the standard deviations of the atomic coordination of our refinements.

Single-Crystal Refinements

Refinements were carried out using the least-squares program LINEX (*12*), and the quantity minimized was $\Sigma W (F_o^2 - k^2F_c^2)^2$ with $W = 1/(\sigma^2(\text{counting}) + (pF_o^2)^2)$. The scale factor is k, and p is a variable weight-

TABLE I

AGREEMENT FACTORS $R = \Sigma|F_o - F_c|/\Sigma|F_o|$, POSITIONS AND THERMAL PARAMETERS FOR SOME OF THE MODELS[a]

	Room temperature		Synthetic crystal (590°C)		Natural crystal (590°C)		Powder (630°C)	
	This work	Le Page and Donnay (*1*)	O in 6*j*	O general	O in 6*j*	O general	O in 6*j* Si in 3*c*	O general Si in 6*g*
Silicon								
X	0.4701(1)	0.46987(9)	½	½	½	½	½	0.486
B							1.95(6)	1.46(9)
U_{11}	0.0056(2)	0.0066(1)	0.0216(9)	0.0227(6)	0.0248(8)	0.0250(6)		
U_{22}	0.0039(2)	0.0051(2)	0.0161(10)	0.0184(6)	0.0190(10)	0.0196(7)		
U_{33}	0.0052(2)	0.0060(1)	0.0166(9)	0.0167(4)	0.0185(9)	0.0178(6)		
U_{12}	½ U_{22}	½ U_{22}	½ U_{22}	½ U_{22}	½ U_{22}	½ U_{22}		
U_{13}	½ U_{23}	½ U_{23}	0	0	0	0		
U_{23}	−0.0006(2)	−0.0003(1)	0	0	0	0		
Oxygen								
X	(0.4136(1)	0.4141(2)	2*Y*	0.4164(3)	2*Y*	0.4168(4)	2*Y*	0.4179(4)
Y	0.2676(1)	0.2681(2)	0.2072(26)	0.2381(11)	0.2072(23)	0.2380(12)	0.2091(2)	0.2432(8)
Z	0.1191(1)	0.1188(1)	⅙	0.1419(10)	⅙	0.1408(11)	⅙	0.1416(8)
U_{11}	0.0137(2)	0.0156(4)	0.0508(13)	0.0529(8)	0.0538(13)	0.0536(9)	0.046(2)	0.051(2)
U_{22}	0.0093(2)	0.0115(3)	0.0531(16)	0.0374(11)	0.0570(20)	0.0406(23)	0.060(11)	0.041(9)
U_{33}	0.0109(1)	0.0119(3)	0.0607(12)	0.0381(23)	0.0630(14)	0.0377(24)	0.035(1)	0.027(7)
U_{12}	0.0078(1)	0.0092(3)	½ U_{11}	0.0298(4)	½ U_{11}	0.0308(7)	½ U_{11}	0.032(2)
U_{13}	−0.0030(1)	−0.0029(3)	0	−0.0064(8)	1	−0.0057(8)	0	−0.002(2)
U_{23}	−0.0048(1)	−0.0046(2)	−0.363(8)	−0.0174(6)	−0.0368(9)	−0.0169(14)	−0.024(3)	−0.013(6)
R %	1.9	1.6	5.3	3.8	5.3	3.5		
R_p (%)							8.04	7.24
R_I (%)							4.40	2.61

[a] The unit cells used are: room temperature (*21*): $a = 4.9134$ Å, $c = 5.4052$ Å. Space group: $P3_221$. 590°C (*22*): $a = 4.9977$ Å, $c = 5.4601$ Å. Space group: $P6_222$.

ing parameter. Final calculations varying p gave only small changes in agreement factors and a value of $p = 0.02$ was finally adopted. The extinction correction was done using the theory of Becker and Coppens (*13*) with the formalism of Thornley and Nelmes (*14*) whenever anisotropic extinction was applied. Extinction was severe for the synthetic crystal. For the room-temperature data a slightly better agreement was obtained when an anisotropic extinction model was used, whereas this was not the case for the high-temperature data. In no case were there any significant variations of the parameters with the various extinction models. The extinction was of the same order of magnitude at the two temperatures, and the largest reduction factor was 0.35 for the reflection 01.1. For the natural crystal the extinction was negligible, the largest reduction being 0.94 for the reflection 01.1.

For the room-temperature data a preliminary estimate of the Dauphiné twinning indicated it to be less than 1%. If there is no extinction and x is fixed we can solve for $F(hkl)_I$ or likewise for $x \ll 1$ we can solve for $|F(hk \cdot l)_I|$ if we replace $|F(kh \cdot l)_{II}|$ by the calculated value, which does not suffer from extinction. This was done for a series of x up to 1% and a minimum in the agreement factor was obtained for an x value of 0.25%. This value was then used in further refinements. Measurements of a few reflections on the natural crystal at room temperature showed x to be near 50%.

For refinement of the room-temperature data, the starting parameters as well as the coordinate system were as given by Le Page and Donnay (*1*) and the results are summarized in Table I. For the high-temperature data, several models were refined to investigate the possible disorder in both the silicon and oxygen atoms. Starting parameters for confined ordered models were those of Young for quartz at 600°C, and for the disordered models those obtained from the powder profile refinement. The results are given in Table I. For Si the thermal motion of the atom placed in the special position $3c$ ($\frac{1}{2}$, 0, 0) was so isotropic that there was no reason to suspect any disorder. Confining the oxygen atom to the special position $6j$ ($2x$, x, $\frac{1}{6}$), however, produced an atomic density strongly smeared along a line connecting the two possible oxygen sites in the twinned low-temperature structure. A much better agreement was obtained when placing the two half-oxygen atoms in general symmetric positions corresponding to α_1 and α_2 sites, although no such improvement was obtained in the case of the silicon atoms. It is possible that a cumulant description of the atomic distribution of oxygen might give an even better agreement. Indeed we obtain some additional improvement using a three-position disorder model for oxygen covering a distribution over the special and general sites. However, it is not possible to refine the occupation factor for these sites without independent determination of the thermal ellipsoids. Nevertheless the present results clearly show that a disorder model is a better description than the ordered model suggested by Young.

The list of structure factors is available in the microfiche version[1] or from the authors.

α-Quartz

The room-temperature structure is in good agreement with the recent study by Le Page and Donnay (*1*) as seen from Table I. The only important differences are found

[1] Order from ASIS/NAPS c/o Microfiche Publications, P.O. Box 3513, Grand Central Station, New York, New York 10163. Remit in advance for each NAPS Accession number. Institutions and organizations may use purchase orders when ordering; however, there is a billing charge for this service. Make checks payable to Microfiche Publications. Photocopies are $5.00. Microfiche are $3.00. Outside of the U.S. and Canada, postage is $3.00 for a photocopy or $1.50 for a fiche.

in the thermal parameters where the X-ray results are consistently larger than the neutron observation. This can be explained by assuming that the thermal parameters of the X-ray data to a certain extent make up for the electronic deformations that occur by bonding, and which are not included in the form factors. It is also possible that the different experimental techniques lead to discrepancies. The amount of thermal diffuse scattering measured is not the same in the two cases, and multiple scattering is undoubtedly of importance in the neutron case as judged from the rather strong extinction. The latter effect would tend to shift intensity to the weak reflections which are mainly found at high angles and therefore the temperature factors would be too small. However, we see no trace of multiple scattering in the extinct 00*l* reflections. Presently a charge density study using the X-ray data is under way (*1*), and this will give us a clear indication whether the whole difference can be explained from charge distortions.

β-Quartz

The most detailed X-ray diffraction study of the $\alpha \rightarrow \beta$ quartz transition was made by Young (*2*), who considered in detail the question of Dauphiné twinning. On the basis of the intensities of a number of chosen reflections in the α- and β-phases it was concluded that β-quartz was not disordered. The structure was defined by a single potential minimum, although this was probably somewhat less than parabolic for oxygen atoms in the direction perpendicular to the Si–O–Si plane. The neutron diffraction refinements in the present work, which take advantage of the larger neutron scattering length of oxygen compared to that of silicon to give greater contrast at the oxygen atom, favor a disordered model based on split-half-oxygen positions. Arnold (*5*) has already proposed that β-quartz is submicroscopically twinned according to the symmetry of α-quartz, but his X-ray film data were not of sufficiently high quality to contest the report of Young. Due to problems of computation Young was not able to test directly his data against the split-atom model although he made an attempt to do so. More recently van Tendeloo *et al.* (*4*) have suggested that the oscillating boundary observed between twin domains in α-quartz just below the phase transition is a time average of α_1 and α_2 domains. The volume swept by this boundary increases with temperature until the microstructure appears homogeneous to the resolution of the electron microscope at the temperature of the β-phase, and they conclude that β-quartz is a time average of the α_1 and α_2 structures. On the basis of these data alone, there is a weakness in this argument because in order to reverse the twin configurations $\alpha_1 \rightleftarrows \alpha_2$ the structure must pass at least momentarily through the ideal β-quartz configuration of Young. The stability of the domain structure in α-quartz shows that the time spent in the α_1 and α_2 configurations is large compared to that spent in the ideal β-quartz configuration which is indicated by the thickness of the twin boundary at any instant of time. Diffraction intensities being defined by the space time average of the structure clearly show in the present work that the average time spent in the α_1 and α_2 configurations at 590°C dominates over that spent in the ideal β-quartz configuration.

Diffraction results do not distinguish between a spatially static microdomain structure, or a time-averaged structure, but diffuse scattering (*4, 15*), intense near the transition and persisting into the β-phase, is inelastic and therefore dynamic in origin (*16, 17*). The diffuse scattering pattern is compatible with the mode which drives the $\alpha \rightarrow \beta$ phase transformation (*4, 18*). Dynamic disorder of oxygen atoms between α_1 and α_2 configurations would normally be

TABLE II

ANGLES AND DISTANCES IN THE SiO_4 UNIT[a]

Model	Si–O (Å)	⟨O–Si–O (deg)		⟨Si–O–Si (deg)
Room temperature	1.608(1) 1.610(1)	110.54(4) 108.74(4)	108.87(4) 109.42(4)	143.61(4)
590°C oxygen in 6*j* position	1.589(9) 1.590(9)	111.3(5) 107.0(5)	110.1(5) 111.3(5)	153.1(2)
590°C oxygen in general position	1.640(5) 1.560(5)	110.3(5) 103.7(3)	109.6(3) 112.8(3)	150.1(2)
590°C oxygen in general position; silicon at 0.484, 0, 0	1.591 1.606	110.5 108.2	108.0 109.8	150.9

[a] Values are given only for the synthetic single crystal. For the 590°C structures the space group $P3_221$ has been used for the calculation assuming that the SiO_4 unit moves as a whole in the case where there is disorder.

coupled with a silicon motion to avoid distortion of the tetrahedral bonds. The calculated bond lengths and angles between a set of α_1 or α_2 oxygen sites and the high-symmetry β-quartz silicon site (Table II) show a distortion of the tetrahedron around silicon. This distortion can be relieved by moving the silicon away from the special position. Figure 1 shows a stereographic picture of the unit cell content, and the motion of relaxation for the silicon in the SiO_4 group is along the twofold axis which is nearly orthogonal to the plane of the figure. By distance and angle calculations involving one-half of the disordered oxygens we find that the distortion is minimized for silicon on $x, y, z = 0.5 \pm 0.016, 0, 0$. Distances and angles in this SiO_4 tetrahedron are given in Table II. In the figure this corresponds to the silicon being above the plane when associated with the dotted oxygen atoms and below when associated with the white oxygen atoms, corresponding again to the α_1 and α_2 twin configurations. The displacement of silicon corresponds to ± 0.08 Å, which is observed as a small anisotropy in the temperature parameters from the single-crystal data. For the powder analysis, where isotropic temperature parameters were used, a similar displacement ($x = 0.5 \pm 0.014$) was found.

We are now in a position to describe the structure of β-quartz. The evidence indicates that the high-symmetry displacive limit of the ideal β-quartz is not achieved as a stable structure. Instead the Dauphiné twin structure of α-quartz below the transition becomes correlated over shorter distances giving an average structure, probably of a dynamic nature. The displacements relating the domains are those of the classi-

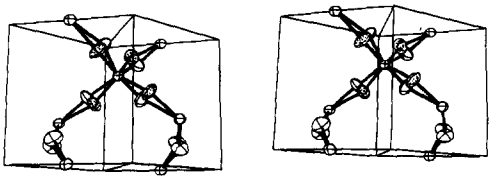

FIG. 1. Stereoview of the unit cell content of β-quartz at 590°C. Small atoms are silicon; large atoms are oxygen. The ellipses enclose regions where the atomic density is higher than 50%, and indicate in this way the average thermal motion and disorder. In the present case the oxygen distribution is represented by two half-atoms. Dotted oxygen atoms correspond to one position of the SiO_4 tetrahedra, and the motion of the tetrahedra can be described as a screw motion along an axis through silicon and approximately orthogonal to the plane of the figure.

cal $\alpha \rightarrow \beta$ phase transition, with an additional twofold symmetry about the ideal β-quartz positions. As is clearly observable in Fig. 1, the displacements describe a screw motion which appears as an undamped overshoot $\alpha_1 \overset{\beta}{\leftrightarrow} \alpha_2$.

Provided the motion is correlated, the SiO_4 tetrahedra are not distorted, so the amplitudes are large and the restoring forces are probably small. The motion will therefore be on a much longer time scale than typical thermal vibrations, corresponding to a very low frequency lattice mode, propagated as a wave through the crystal (Tendeloo *et al.* (*4*)). Transient occupancy of the ideal β-quartz sites is implicit in this model, but the local α-quartz symmetry is dominant.

Comparison with High-Temperature Silica Polymorphs

Disorder has been recognized in two other important crystalline polymorphs of silica, both of which are high-temperature forms related to an ordered structure by a rapid displacive transition. β-Cristobalite has been shown to have 16 oxygen atoms distributed over the 96 (h) positions in the cubic space group $Fd3m$ (*19*). This average structure is interpreted in terms of a short-range order in domains of lower symmetry with each domain a subset of 16 sites of 96 (h) of $Fd3m$, each occurring with equal probability. The subset of 16 positions is a set of $F\bar{4}d2$, or taking the smaller tetragonal cell $I\bar{4}2d$, which compares directly with α-cristobalite, reduces to the set 8d of $I\bar{4}2d$. Disorder of the silicon atoms in β-cristobalite has also been noted (*19*), but has simply been described as relaxation of the Si atoms to relieve stress on the silica tetrahedral angles caused by the displacements at domain boundaries. The domain structure represents a sixfold microtwinning of the tetragonal cell to generate the average structure, and consequently any small silicon disorder appears as an increased isotropic thermal parameter. It is evident, however, that the disorder in β-cristobalite may also be a correlated displacement of the silicon and oxygen atoms toward the α-cristobalite position of the six twin configurations, in which case the local structure in each domain has α-cristobalite symmetry ($P4_12_12$). The cristobalite and quartz transformations are then very closely related. Although the common twinning operation in α-cristobalite is only twofold, with increasing temperature the axial ratio c_0/a_0 moves from 0.986 $(2)^{1/2}$ to $2^{1/2}$. This gives the additional possibility of threefold twinning about the body diagonal of the pseudo cubic unit cell, and an average unit cell of cubic symmetry with sixfold-disorder β-cristobalite.

The structure of orthorhombic high tridymite is also disordered relative to that of ideal high tridymite (*20*). SiO_4 tetrahedra are twisted and adjacent tetrahedra alternatively displaced in the b-axis direction. The oxygen atoms show strong thermal motion normal to the Si–O–Si plane. Electron density maps demonstrate clearly the elongated oxygen position and confirm that the oxygen atom is disordered.

Taken altogether, the results on β-quartz, β-cristobalite, and β-tridymite indicate a general instability of the high-symmetry SiO_2 structures compared to disordered structures of lower local symmetry. This instability is due to the freedom of rotation (even over a limited range) of the silica tetrahedra about the twofold axes without distortion of the SiO_4 tetrahedra. Only in β-cristobalite, however, is this freedom exploited along all three axes. In β-quartz and β-tridymite the crystal symmetry restricts the rotation to only one twofold axis of the tetrahedra.

This work is being continued as a study of the thermal and structural parameters of quartz from 500 to 1000°C.

Acknowledgments

We thank Professor R. Cowley and Drs. B. Dorner and R. Pynn for helpful suggestions and discussions. Professor G. Donnay is thanked for critical reading of the manuscript and many helpful comments. We are indebted to Mr. J. Allibon for very efficient technical support.

References

1. Y. LE PAGE AND G. DONNAY, *Acta Crystallogr. Sect. B* **32**, 2456 (1976).
2. R. A. YOUNG, Armed Services Technical Information Agency Report No. AD 276235, Arlington, Va. (1962).
3. G. DOLINO AND J. P. BACHHEIMER, *Phys. Status Solidi A* **41**, 673 (1977).
4. G. VAN TENDELOO, J. VAN LANDUYT, AND S. AMELINCKX, *Phys. Status Solidi A* **33**, 723 (1976).
5. H. ARNOLD, *Z. Kristallogr.* **117**, S467 (1962).
6. A. J. LEADBETTER AND A. F. WRIGHT, *Phil. Mag.* **33**, 1, 105 (1976).
7. H. M. RIETVELD, *J. Appl. Crystallogr.* **2**, 65 (1969).
8. R. ARGOUD, J. J. CAPPONI, J. CHENAVAS, M. MAREZIO AND L. PONTONNIER, Fourth European Crystallography Meeting, Oxford, England (1977).
9. M. S. LEHMANN AND F. K. LARSEN, *Acta Crystallogr. Sect. A* **30**, 580 (1974).
10. A. W. HEWAT, *Phys. Lett. A* **39**, 249 (1972).
11. G. E. BACON, *The Neutron Diffraction Newsletter* (W. B. Yelon, Ed.), February (1977).
12. P. COPPENS, private communication (1975).
13. P. BECKER AND P. COPPENS, *Acta Crystallogr. Sect. A* **30**, 129 (1974).
14. F. R. THORNLEY AND R. J. NELMES, *Acta Crystallogr. Sect. A* **30**, 748 (1974).
15. H. ARNOLD, *Z. Kristallogr.* **121**, 145 (1965).
16. K. H. W. BAUER, H. JOGODZINSKI, B. DORNER, AND H. GRIMM, *Phys. Status Solidi B* **48**, 437 (1971).
17. J. D. AXE AND G. SHIRANE, *Phys. Rev. B* **1**, 1, (1970).
18. H. GRIMM AND B. DORNER, *J. Phys. Chem. Solids* **36**, 407 (1975).
19. A. F. WRIGHT AND A. J. LEADBETTER, *Phil. Mag.* **31**, 1391 (1975).
20. W. A. DOLLASE, *Acta Crystallogr.* **23**, 617 (1967).
21. A. J. COHEN AND G. G. SUMNER, *Amer. Min.* **43**, 58 (1958).
22. R. J. ACKERMANN AND SUMNER, C. SORREL, *J. Appl. Crystallogr.* **7**, 461 (1974).